ORIGINAL PAPER

GLI1-Altered Soft Tissue Tumors of the Head and Neck: Frequent Oropharyngeal Involvement, p16 Immunoreactivity, and Detectable Alterations by *DDIT3* Break Apart FISH

Doreen N. Palsgrove[1,8] · Lisa M. Rooper[2] · Todd M. Stevens[3] · Christina Shin[4] · Douglas D. Damm[5] · Jeffrey Gagan[1] · Julia A. Bridge[6] · Lester D. R. Thompson[7] · Prasad R. Koduru[1] · Justin A. Bishop[1]

Abstract

Background GLI1 is a transcription factor protein that has recently gained recognition in a morphologically distinct group of epithelioid soft tissue tumors characterized by *GLI1* fusions or amplifications. The head and neck region, particularly the tongue, is a common location for *GLI1*-altered tumors. *DDIT3* break apart fluorescence in situ hybridization (FISH), commonly used to identify translocations in myxoid/round cell liposarcoma, has been used as a surrogate test to detect both fusions and amplifications of the 12q13.3 region encompassing *DDIT3* and *GLI1* gene loci.

Methods We herein report 5 cases of *GLI1*-altered soft tissue tumors. Three arose in the oropharynx (base of tongue/vallecula, tonsil) and two arose in the tongue. Given the frequent oropharyngeal location and epithelioid morphology, p16 immunohistochemistry was performed on cases with available material. Commercially available *DDIT3* break apart FISH, custom *GLI1* specific FISH, and RNA sequencing were performed on select cases.

Results Two cases showed amplification using *DDIT3* FISH which was confirmed using *GLI1* specific FISH. The remaining cases harbored *ACTB::GLI1*, one of which showed rearrangement of the 12q13.3 region by *DDIT3* FISH with absence of amplification by *GLI1* specific FISH. STAT6 immunoexpression was positive in the *GLI1*-amplified cases and negative in the *GLI1*-rearranged cases while MDM2 expression was positive in the 4 cases tested. CDK4 expression was strong and diffuse in the *GLI1*-amplified cases. p16 immunohistochemistry showed strong nuclear and cytoplasmic staining in 50–70% of tumor cells in all four tested cases.

Conclusion Here we show that *GLI1*-altered soft tissue tumors are frequently positive for p16 and can occur in tonsillar regions of the oropharynx. As such, positive p16 immunohistochemistry alone cannot be used as evidence for the diagnosis of HPV-related squamous cell carcinoma as strong and diffuse p16 expression may also occur in *GLI1*-altered soft tissue tumors. Commercially available *DDIT3* break apart FISH, which is readily available in many cytogenetic laboratories, may be useful as a sensitive surrogate test for *GLI1* fusions and amplifications.

Keywords *GLI1* · Oropharynx · p16 · *DDIT3* · FISH

✉ Doreen N. Palsgrove
doreen.palsgrove@utsouthwestern.edu

1 Department of Pathology, University of Texas Southwestern Medical Center, Dallas, TX, USA

2 Department of Pathology, Johns Hopkins University School of Medicine, Baltimore, MD, USA

3 Department of Pathology, University of Kansas Medical Center, Kansas City, KS, USA

4 Histopathology Department, Middlemore Hospital, Auckland, New Zealand

5 Pathology and Cytology Laboratories, Lexington, KY, USA

6 ProPath, Dallas, TX, USA

7 Head and Neck Pathology Consultations, Woodland Hills, CA, USA

8 UT Southwestern Medical Center, Clements University Hospital UH04.234, 6201 Harry Hines Boulevard, Dallas, TX 75390, USA

Introduction

GLI1 fusions and amplifications are the main oncogenic events that characterize a subset of epithelioid soft tissue (mesenchymal) tumors with a predilection for the head and neck [1–4]. Most are characterized by monomorphic epithelioid and/or spindled cells and are frequently associated with a rich vascular network. Immunohistochemistry has thus far been unreliable for diagnosing these tumors. Even targets that reside near the *GLI1* gene locus on chromosome 12p, including *CDK4*, *MDM2*, and *STAT6* on chromosome 12q13–15, are not entirely sensitive, especially for tumors harboring a rearrangement [1]. As a result, molecular confirmation of a fusion or amplification involving the *GLI1* locus is typically required for definitive diagnosis.

Most *GLI1*-altered soft tissue tumors reported in the head and neck region have occurred in the tongue or soft tissue of the neck with rare cases in the floor of mouth [2]. The oropharynx is a lesser-known affected site, with only three cases reported to date: two in the base of tongue (one with extension to the right oral tongue and lateral pharyngeal wall) and one soft palate (with extension to the lateral nasopharyngeal wall) [2–4].

Here, we describe five additional cases of *GLI1*-altered soft tissue tumors, including oropharyngeal primaries, and characterize the extent and pattern of p16 expression by immunohistochemistry.

Materials and Methods

Cases

Cases of *GLI1*-altered soft tissue tumors were retrieved from the consultation and/or institutional files of three authors (JAB, LMR, and LDRT). Hematoxylin and eosin-stained slides from all cases along with previously performed immunohistochemical stains were reviewed. Additional immunohistochemical studies were performed on select cases using a monoclonal antibody directed against p16 utilizing standard techniques. This study was approved by the Institutional Review Boards at our respective institutions. Four cases (cases 1 to 4) are new while case 5 was previously reported [1, 5].

Fluorescence In Situ Hybridization (FISH)

DDIT3 FISH was performed on 3 of 5 cases using either: (1) the Vysis (Abbott, Abbott Park, Illinois, USA) LSI (12q13) dual color, break apart DNA probe set; and/or (2) the Cyto-Cell (Oxford Gene Technology, Cambridge, UK) dual color,

break apart DNA probe set. A custom *GLI1* locus spanning probe coupled with CEN12 (copy number control) was used to assess for *GLI1* specific amplification in cases with available material.

RNA Sequencing

Case 2 was subjected to a custom, clinically validated NanoString fusion assay [6] while Case 3 underwent a Sarcoma Targeted Gene Fusion/Rearrangement Panel (Mayo Clinic). Targeted RNA sequencing (RNA-seq) was performed on Case 4 at the UTSW NGS Clinical Lab at the Once Upon a Time Human Genomics Center. Briefly, whole-slide tissue sections were cut at 10 μm, and Qiagen AllPrep kits (Qiagen, Germantown, MD) were used for RNA isolation. A sequencing library was generated using a modified TruSight RNA Pan-Cancer kit (Illumina, San Diego, CA) with 1425 genes. Sequencing was performed on the NextSeq 550 (Illumina, San Diego, CA) with a minimum of 6 million mapped reads. Fusions were called using the Star-Fusion algorithm [7] and were manually reviewed via the Integrated Genomics Viewer (Broad Institute, Cambridge, MA).

Results

Clinicopathologic Findings

Clinicopathologic information is summarized in Table 1. The patients ranged in age from 35 to 84 years, all males. Tumors ranged from 15 to 60 mm in greatest dimension. Locations included the oropharynx (Figs. 1, 2, and 3: 1 tonsil, 1 base of tongue/vallecula, 1 not otherwise specified) and tongue (Figs. 4 and 5: 1 left dorsal tongue, 1 left ventral tongue). Incisional or excisional biopsies for routine diagnosis were reviewed, with one case obtained by radical tonsillectomy with partial resection of the posterior pharyngeal wall.

Histologically, tumors were predominantly composed of relatively monomorphic oval shaped cells with clear to pale, eosinophilic cytoplasm, delicate speckled chromatin, and small variably conspicuous nucleoli (Figs. 2, 3, 4, and 5) with the exception of one case which demonstrated a cellular multinodular spindle cell proliferation arranged in loose fascicles within a variably myxoid to hyalinized stroma with dilated vessels (Fig. 1). However, focally the tumor cells were more epithelioid and nested with a prominent capillary vasculature (Fig. 1E–F). At low power, tumors appeared to be relatively circumscribed, but at higher power demonstrated varying degrees of infiltration at the periphery. A fine vasculature with peritheliomatous tumor cell arrangement in vague nodules and anastomosing cords

Table 1 Clinicopathologic, immunophenotypic, and molecular characteristics of *GLI1*-altered soft tissue tumors in the current study

Case	Age/Sex	Site (Size)	STAT6 IHC	MDM2 IHC	CDK4 IHC	P16 IHC	CytoCell *DDIT3* FISH	Vysis *DDIT3* FISH	*GLI1* FISH	RNA seq
1	35/M	Right tonsil (1.5 cm)	Weak, focally+	Moderate, diffuse	Strong, diffuse	>70%, Strong	NP	Amplified	Amplified	NP
2	84/M	Right base of tongue/val-lecula (unknown)	–	Patchy+	NP	50%, Strong	NP	NP	NP	*ACTB::GLI1*
3	53/M	Left oropharynx (6 cm)	–	NP	NP	NP	NP	NP	NP	*ACTB::GLI1*
4	41/M	Left dorsal tongue (unknown)	Weak, focally+	Weak, diffuse	Weak, focally+	50%, Strong	Rearranged	Rearranged	Not amplified	*ACTB::GLI1*
5*	65/M	Left ventral tongue (2 cm)	Moderate, diffuse	Moderate, diffuse	Strong, diffuse	>70%, Strong	NP	Amplified	Amplified	NP

NP not performed

*Previously published

was common. Protrusion of tumor nests into vascular spaces was seen in only one case (Fig. 4). Collagenous stroma was present in varying amounts in all cases but was most notable in Case 1 (Fig. 1A–C). Four cases showed overlying mucosal ulceration. Infiltrating lymphocytes were not prominent. Mitotic activity was moderate in one case (Case 1; 5–7 mitoses/2 mm^2). Perineural invasion and necrosis was uniformly absent.

All cases tested by immunohistochemistry showed at least focal expression of CDK4 (3/3) and MDM2 (4/4), while STAT6 was variable (negative–2; weak, focal–2; moderate, diffuse–1). Case 1 was additionally positive for bcl-2, GLUT1, vimentin, and CD56, focally positive for CK8/18 and CD34, and negative for EMA, CD21, CD23, AR, PR, chromogranin, synaptophysin, neurofilament, AE1/AE3, CD99, WT1, ALK1, S100 protein, SOX10, GFAP, caldesmon, calponin, SMA, CD31, ERG, CK5/6, CK14, p63, p40, and beta-catenin. Given the anatomic location and epithelioid morphology, p16 immunohistochemistry was performed on two oropharyngeal cases with available material (Case 1 and 2) and showed strong nuclear and cytoplasmic block-like staining in 50–70% of tumor cells; the ventral and dorsal tongue tumor cases demonstrated similar p16 results (Table 1).

Molecular Alterations

RNA-seq showed *ACTB*::*GLI1* fusion in 3 of 5 tumors (Case 2–4). *DDIT3* break apart FISH was performed on 1 of the cases with *GLI1* fusion (Case 4) and was positive for rearrangement of the 12q13.3 region using both the CytoCell and Vysis probe sets while *GLI1* specific FISH was negative for *GLI1* amplification (Fig. 4G). Cases 1 and 5 were positive for amplification by custom *GLI1* specific FISH and Vysis *DDIT3* FISH. Case 1 additionally demonstrated increased copy numbers of *MDM2* (Zytovision ZytoLight SPEC, IGENZ, Auckland, NZ) and *GLI1* using Kreatech Poseidon FISH probes (IGENZ, Auckland, NZ) but no rearrangement of *SS18* (Vysis).

Discussion

GLI1-altered soft tissue tumors characteristically harbor either fusions (most commonly involving *ACTB*, *MALAT1,* and *PTCH1* gene partners) or high-level amplifications of the *GLI1* locus, frequently accompanied by co-amplification of other genes mapped to the chromosome 12q13–q15 region (e.g., *MDM2*, *CDK4*, *DDIT3*, and *STAT6*). Patients across a wide age range (1–88 years) may present with tumors arising in bone and soft tissue [5, 8, 9], skin [10], lung [5], genitourinary system [8, 11, 12], gastrointestinal tract [13, 14], oral cavity [1, 2, 5, 13], or oropharynx [2–4].
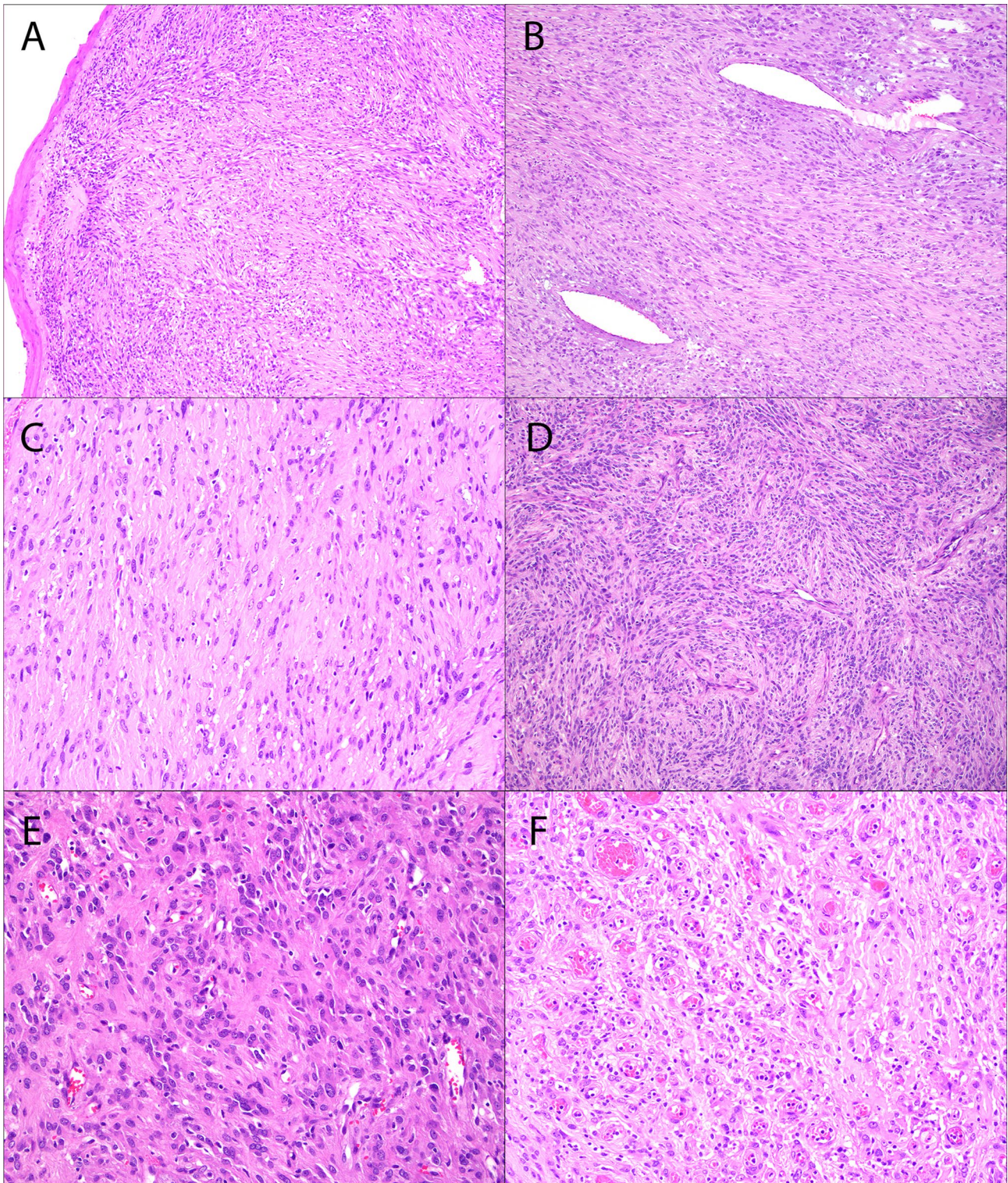
Fig. 1 Right palatine tonsil *GLI1*-amplified soft tissue tumor (Case 1). The tonsil is effaced by a cellular multinodular spindle cell proliferation arranged in loose fascicles (**A**, **B**, **C**, **D**) within a variably myxoid to hyalinized stroma, reminiscent of a nerve sheath tumor, solitary fibrous tumor, or monophasic synovial sarcoma. The tumor cells contain abundant eosinophilic cytoplasm and oval to spindled nuclei with mild nuclear pleomorphism. Additional features include dilated vessels (**B**), a sprinkling of intratumor lymphocytes, and focal epithelioid morphology (**E**, **F**) with a prominent capillary vasculature (**F**)
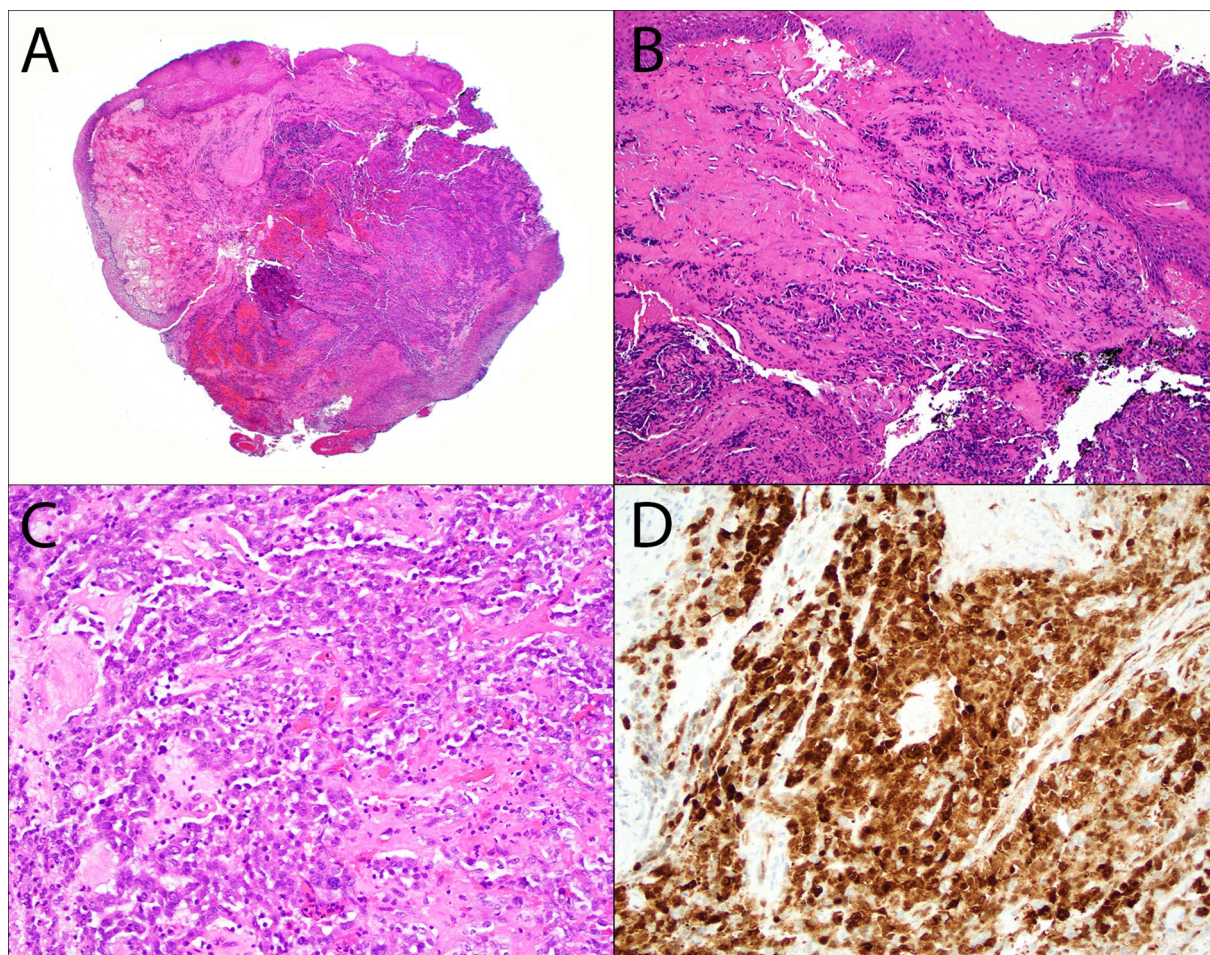
Fig. 2 Base of tongue *ACTB*::*GLI1* fusion-related soft tissue tumor (Case 2). A cellular proliferation of epithelioid cells arranged in nests and anastomosing trabecula (**A–C**) is seen beneath an ulcerated mucosal surface (**A**). Hyalinized stroma is variably present (**B**, **C**) along with occasional intratumoral lymphocytes (**C**). There is strong nuclear and cytoplasmic, block-like p16 immunoexpression in > 70% of tumor cells (**D**)

Morphologically, this tumor family is typically characterized by a monomorphic population of epithelioid and/or spindled cells with a prominent perivascular distribution of growth, reminiscent of pericytic neoplasms. The immunoprofile of *GLI1*-altered soft tissue tumors, however, is known to be highly variable with immunoreactivity for relatively nonspecific markers (cyclin D1, CD10, BCOR, bcl-2) and inconsistent expression of S100 protein, actins, keratins, and neuroendocrine markers. Reported cases with available follow up data suggest these lesions behave similarly to low-grade sarcomas and have around a 20% rate of local recurrence and metastasis to regional lymph nodes and distant sites [1, 2, 4, 8, 14–16]. Tumor-related death was reported in one case arising in the uterus and metastasizing to brain [15].

Although a few cases of oropharyngeal *GLI1*-altered soft tissue tumors have been described [2–4], our series is the first to report one specifically arising in the palatine tonsil (Table 2). The tonsillar regions of the oropharynx (palatine and lingual tonsils) are particularly unique given the rich supply of lymphatics and small blood vessels, "immune privileged" environment, and discontinuous basement membrane of the reticulated epithelium [17, 18]. Tumors arising in these locations are more prone to regional lymph node spread [19]. Although none of the oropharyngeal primaries presented here have any follow up data, Zhong et al., [4] described a *GLI1*-rearranged tumor of the right base of tongue that metastasized to an ipsilateral level II lymph node and contralateral sacral soft tissue. The overall prognosis of head and neck *GLI1*-altered tumors, however, seems to be favorable, despite their potential for local and distant metastases, with no tumor-related deaths reported to date [1, 5].

Our series is the first to report the consistent finding of strong nuclear and cytoplasmic block-like p16 immunoexpression in *GLI1*-altered soft tissue tumors. p16 (INK4a/CDKN2A) is a cell cycle protein that inhibits CDK4, keeping Rb hypophosphorylated and preventing cell cycle

progression. It is typically overexpressed secondary to oncogene-induced senescence or as a mechanism to arrest the uncontrolled proliferation caused by failure of the Rb pathway in tumors. In HPV-related squamous cell carcinoma (SCC), for example, p16 is overexpressed secondary to viral inactivation of Rb leading to the removal of Rb's negative regulation of p16. The significance of increased expression of p16 in *GLI1*-altered tumors is unclear but not entirely unexpected as it is seen in differentiated and de-differentiated liposarcomas [20], which harbor amplifications of the 12q13-15 region encompassing *MDM2* and *CDK4* [5]. Induced expression of p16 inhibits CDK4-associated kinase activity [21] and GLI1 has been shown to directly activate the PI3K/AKT pathway and subsequently

Fig. 4 Dorsal tongue *ACTB*::*GLI1* fusion-related soft tissue tumor ▶ (Case 4). Infiltrating lobules of epithelioid cells can be seen infiltrating beneath the epithelium (**A**–**C**) and protruding into a superficial blood vessel (**A**). Myxoid change with microcyst formation is focally present (**B**). Tumor cells are arranged in a perivascular distribution around intratumoral blood vessels (**D**–**E**). Strong nuclear and cytoplasmic block-like p16 immunoexpression seen in 50% of tumor cells (**F**). *DDIT3* FISH (CytoCell break apart probe set; green 165 kb probe 5′ to the *DDIT3* gene locus and red 146 kb probe 3′ to the *GLI1* gene locus) was positive for rearrangement of the 12q13.3 region (G, left-hand image, arrows indicate the cells with split red and green signals). Custom FISH probe specifically spanning the *GLI1* locus coupled with a CEN12 FISH probe was negative for *GLI1* specific amplification (G, right-hand image, arrows indicate cells with two CEN12 signals and three *GLI1* signals including split of at least one of the *GLI1* signals secondary to rearrangement involving the *GLI1* specific locus)
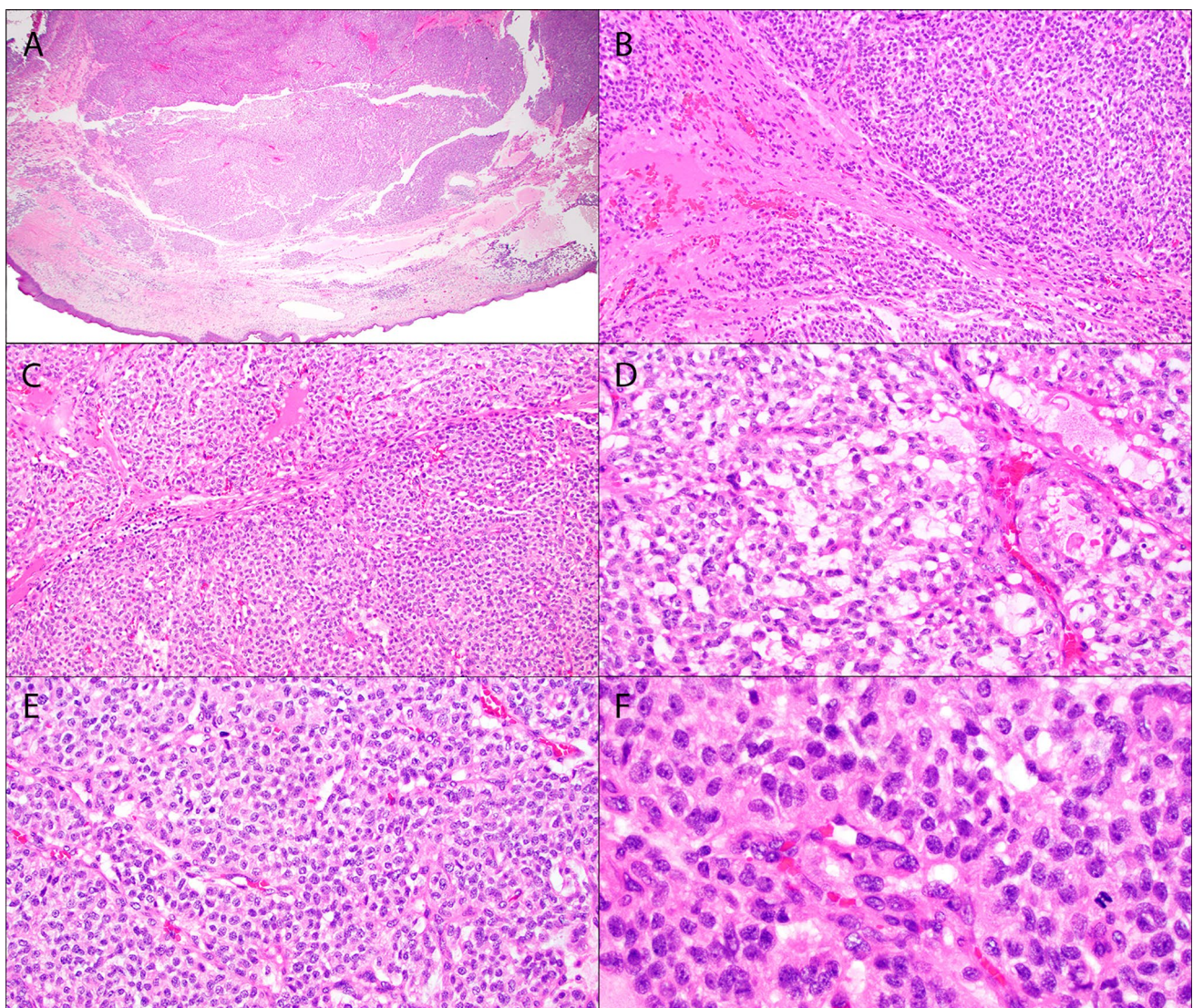

Fig. 3 Oropharynx *ACTB*::*GLI1* fusion-related soft tissue tumor (Case 3). Low power shows expanded nodules of monotonous epithelioid cells (**A**–**C**). Variably hyalinized stroma is seen between some of the lobules (**B**–**C**). Within the nodules, an arborizing thin-walled vasculature show perivascular tumor cell nests (**D**–**E**). Focal myxoid change with microcysts is noted (**D**). High power view demonstrates round to ovoid nuclei with clear to pale eosinophilic cytoplasm (**F**)
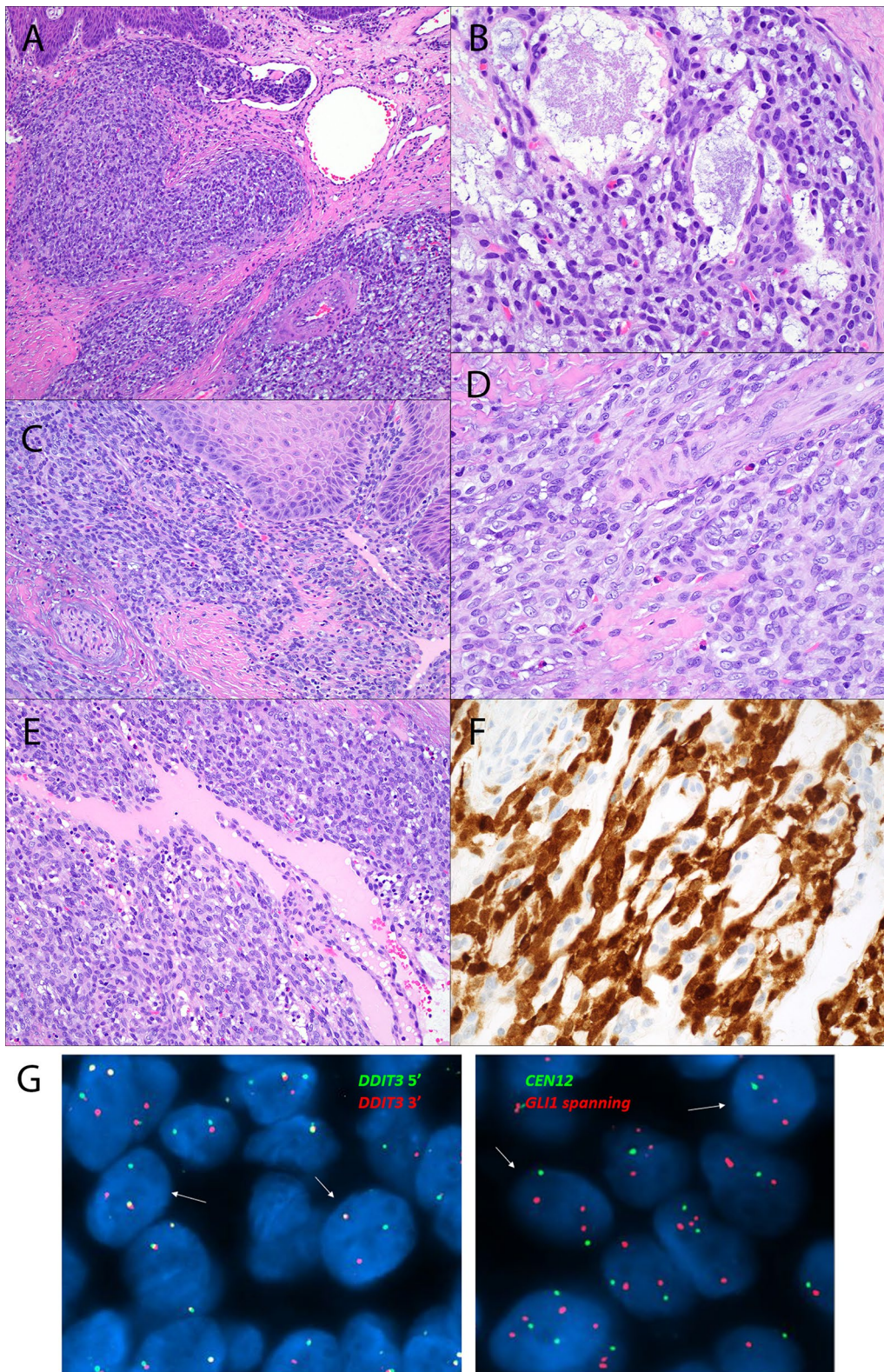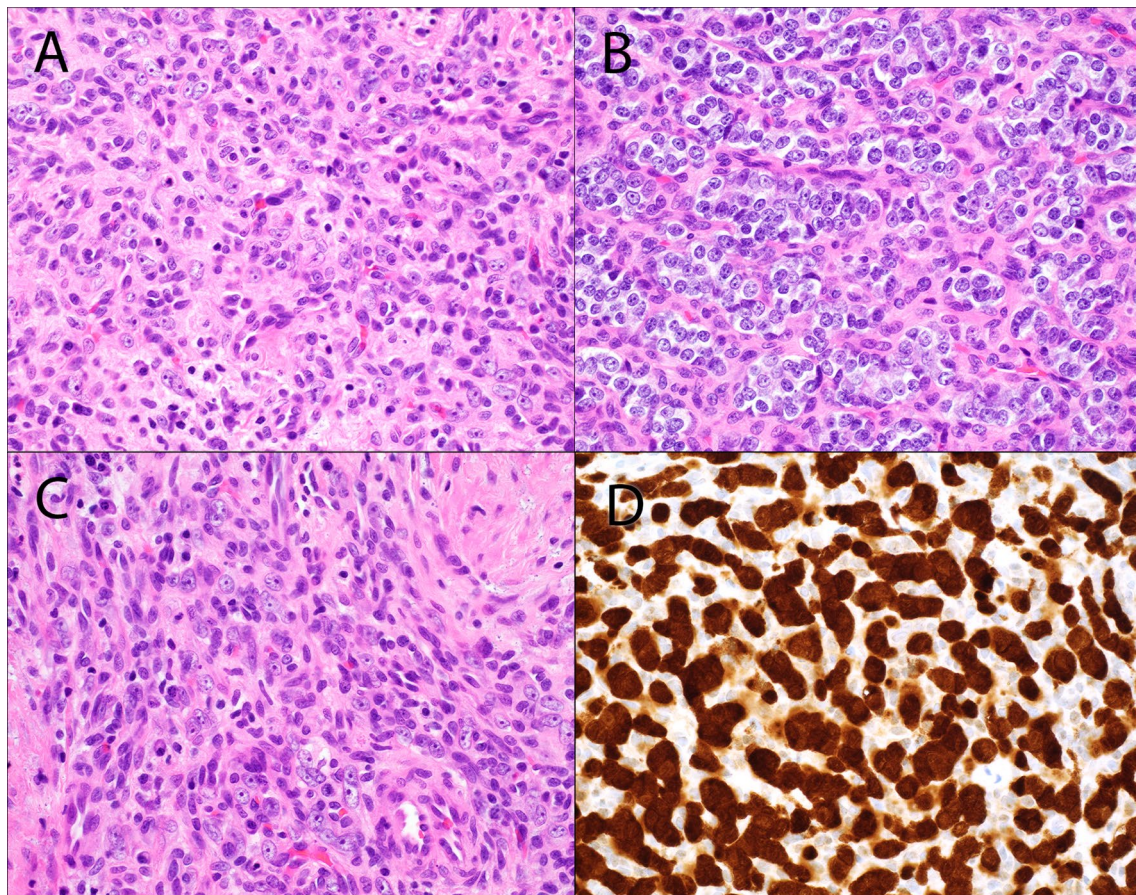
Fig. 5 Ventral tongue *GLI1*-amplified soft tissue tumor (Case 5). Tumor cells are round to focally spindled (**A–C**) and separated by a variably hyalinized fibrovascular stroma. Strong nuclear and cytoplasmic block-like p16 immunoexpression in > 70% of tumor cells (**D**)

up-regulate CDK4/6 protein [22]. GLI1 is also an important Hedgehog pathway transcriptional regulator of genes such as cell cycle regulators *CCND1/2* and *CCNE1* [23]. Therefore, p16 overexpression in *GLI1*-altered tumors could be explained by the concept of induced cellular

senescence in which cancer cells attempt to suppress the G1/S transition driven by *GLI1* induced oncogenic accumulation of cyclins and CDK4. Extended molecular analysis of a *MALAT1*::*GLI1* fusion-related tumor by Prall et al., [14] also detected chromosomal losses involving 13q

Table 2 Literature review of *GLI1*-altered soft tissue tumors primary to the oropharynx

Study	Age/Sex	Site	*GLI1* alteration	Outcome
Current study	35/M	Right palatine tonsil	Amplified	Recent case
Current study	84/M	Base of tongue/vallecula	*ACTB*::*GLI1*	Recent case
Current study	53/M	Oropharynx, not otherwise specified	*ACTB*::*GLI1*	Recent case
Liu et al. [2]	27/M	Tongue base	*ACTB*::*GLI1*	NED (16 months)
Zhong et al. [4]	56/M	Right base of tongue extending to the right oral tongue and lateral pharyngeal wall	*GLI1* rearrangement	- Local metastasis to right level II neck and distant metastasis to left sacrum 27 months after primary tumor resection - NED 36 months after neck dissection, resection of sacral mass, and chemotherapy
Klubíčková, et al. [3]	34/F	Soft palate and lateral nasopharyngeal wall	*PTCH1*::*GLI1*	NED (4 months)

NED no evidence of disease

Table 3 FISH probes used in previous studies for *GLI1*-altered soft tissue tumors

Study	FISH Probes Used	Cytoband	Gene Loci
Antonescu et al. [31] Agaram et al. [5] Argani et al. [15] Liu et al. [2] Xu et al. [1]	Custom break apart BAC clones (RP11-1145D7, RP11-976L20, RP11-112B10)	12q13.3	c-*GLI1-DDIT3*
Antonescu et al. [31] Argani et al. [15]	Custom break apart BAC clones (RP11-936I7, RP11-625C11)	12q13.3	t-*DDIT3*
Agaram et al. [5]	Custom break apart BAC clones (RP11-936I7)	12q13.3–12q14.1	m-*CDK4*/t-*DDIT3*
Agaram et al. [5] Liu et al. [2] Xu et al. [1]	Custom break apart BAC clones (RP11-625C11)	12q13.3	t-*DDIT3*
Zhong et al. [4]	Break apart probe (Anbiping, Guangzhou, China)	12q13.3	*GLI1* (12q13.3)
Pettus et al. [11]	Custom fusion probe set (cocktails of BAC clones spanning GLI1 and FOXO4 gene loci)	12q13.3 and Xq13.1	*GLI1* (12q13.3) and *FOXO4* (Xq13.1)

BAC bacterial artificial chromosome, *t* telomeric, *c* centromeric, *m* covering the gene

(harboring *BRCA2* and *RB1*) and 17p (harboring *TP53*) as well as a truncating *TP53* mutation; thus, one could also anticipate inactivation of *RB1* and/or loss of p53 function leading to p16 overexpression.

In the oropharynx, p16 is used as a surrogate marker for transcriptionally active high-risk HPV in primary oropharyngeal SCCs. Although *GLI1*-altered tumors seem to be morphologically distinctive relative to HPV-related SCCs, if only limited biopsy material is available, one could easily misdiagnose a *GLI1*-altered tumor as a nonkeratinizing HPV-related SCC, or, if there is immunoreactivity for neuroendocrine markers, an HPV-related neuroendocrine carcinoma, which is typically treated with platinum-based chemotherapy. Follicular dendritic cell sarcoma can also occur in the oropharynx and overexpress p16 but would typically stain with dendritic cell markers such as CD21, CD23, and CD35 [24, 25]. Further, given that *GLI1*-altered soft tissue tumors may show hyalinized stroma with monomorphic, low-grade clear cells, hyalinizing clear cell carcinoma, which can also express p16 and arise in the oropharynx [26], could enter the differential diagnosis. The spindled morphology of a subset of *GLI1*-altered soft tissue tumors also overlaps with that of solitary fibrous tumor, a fibroblastic neoplasm with variable clinical behavior that rarely occurs in the oropharynx [27, 28]. Solitary fibrous tumors are distinctly characterized by a recurrent intrachromosomal *NAB2*::*STAT6* fusion with the resultant fusion protein acting as a transcriptional activator through early growth response (EGR)-mediated pathways [29]. Not only do solitary fibrous tumors show increased nuclear immunoexpression of the C terminus of STAT6, a subset of cases may also overexpress p16 [30]. The small number of cases in our series limits the generalizability of p16 overexpression in *GLI1*-altered

tumors but highlights the potential pitfall for misdiagnosis in the oropharynx.

Cases reported in the literature thus far have used a variety of methodologies including targeted exome sequencing [5, 11, 15], RNA sequencing [1–3, 5, 10, 11, 15, 16, 31], and FISH [1, 2, 4, 5, 11, 15, 31]. FISH is frequently the assay of choice when compared to the time and resources required for targeted exome or RNA sequencing; however, it is currently unclear whether a specific *GLI1* targeted probe set is required for detection. FISH analysis thus far has largely been limited to custom bacterial artificial chromosome (BAC) clones flanking the *DDIT3* gene locus with or without *GLI1* (Table 3). The *GLI1* and *DDIT3* gene loci are located near each other on 12q13.3; the distance between the 3′ *GLI1* gene locus (ENST00000228682.7; chr12:57459785-57472268; 12,484 bp) and 3′ *DDIT3* gene locus (ENST00000623876.2; chr12:57516588-57521737; 5,150 bp) is 44,320 bp (44.320 kb). Commercially available FISH break apart probes for *DDIT3* are commonly used to identify translocations involving *DDIT3* associated with myxoid/round cell liposarcoma. The Vysis *DDIT3* break apart FISH probes flank DDIT3 (approximately 134 kb gap) with a 700 kb probe lying proximal to *DDIT3* (spanning *STAT6* and *GLI1* gene loci) and a 663 kb probe extending distally from *DDIT3* (spanning the *CDK4* gene locus), while the CytoCell *DDIT3* break apart FISH probes flank both *GLI1* and *DDIT3* (100 kb gap) with a 146 kb probe lying proximal to *GLI1* and a 165 kb probe extending distally from *DDIT3*. Our experience using these two commercially available *DDIT3* break apart FISH probe sets suggests that it is an effective surrogate for *GLI1*, and that *GLI1* specific FISH probes and custom BAC clones are not needed to diagnose *GLI1*-altered (rearranged or amplified) tumors in routine practice. One limitation of utilizing FISH assays is the possibility of cryptic intrachromosomal inversion events resulting in false negative FISH results,

but these are not yet reported for *GLI1*. For *GLI1*-amplified tumors, *DDIT3* break apart FISH also appears to be sufficient for diagnostic purposes regardless of co-amplification status of neighboring genes (e.g., *STAT6*, *MDM2*, and/or *CDK4*).

In summary, *GLI1*-altered soft tissue tumors can occasionally arise in the oropharynx, show strong nuclear and cytoplasmic block-like p16 immunoexpression, and can be diagnosed using commercially available *DDIT3* break apart FISH. Like many other immunohistochemical markers, p16 expression is nonspecific and should be interpreted with caution in small biopsy material where characteristic histomorphologic features may be obscured or limited.

Data Availability Not applicable.

Code Availability Not applicable.

Declarations

Conflict of interest All authors certify that they have no affiliations with or involvement in any organization or entity with any financial interest or non-financial interest in the subject matter or materials discussed in this manuscript.

Ethical Approval All procedures performed in this retrospective data analysis involving human participants were in accordance with the ethical standards of the institutional review board (IRB 112017-073), which did not require informed consent. All authors confirm they have meaningfully contributed to the research and read and approved the final manuscript.

Consent to Participate Waived by the IRB due to the retrospective nature of the work without therapeutic alterations.

Consent for Publication Obtained from all individual participants for whom identifying information is uniquely included in this manuscript.

References

1. Xu B, Chang K, Folpe AL, Kao YC, Wey SL, Huang HY, et al. Head and neck mesenchymal neoplasms with GLI1 gene alterations: a pathologic entity with distinct histologic features and potential for distant metastasis. Am J Surg Pathol. 2020;44(6):729–37.

2. Liu J, Mao R, Lao IW, Yu L, Bai Q, Zhou X, et al. GLI1-altered mesenchymal tumor: a clinicopathological and molecular analysis of ten additional cases of an emerging entity. Virchows Arch. 2021;480(5):1087–99.

3. Klubickova N, Kinkor Z, Michal M, Baneckova M, Hajkova V, Michalek J, et al. Epithelioid soft tissue neoplasm of the soft palate with a PTCH1-GLI1 fusion: a case report and review of the literature. Head Neck Pathol. 2021;16(2):621–30.

4. Zhong H, Xu C, Chen X, Guo X, Yang S. GLI1-altered epithelioid soft tissue tumor: a newly described entity with a predilection for the tongue. Oral Surg Oral Med Oral Pathol Oral Radiol. 2021;134(1):e14–22.

5. Agaram NP, Zhang L, Sung YS, Singer S, Stevens T, Prieto-Granada CN, et al. GLI1-amplifications expand the spectrum of soft tissue neoplasms defined by GLI1 gene fusions. Mod Pathol. 2019;32(11):1617–26.

6. Haley L, Parimi V, Jiang L, Pallavajjala A, Hardy M, Yonescu R, et al. Diagnostic utility of gene fusion panel to detect gene fusions in fresh and formalin-fixed, paraffin-embedded cancer specimens. J Mol Diagn. 2021;23(10):1343–58.

7. Haas BJ, Dobin A, Li B, Stransky N, Pochet N, Regev A. Accuracy assessment of fusion transcript detection via read-mapping and de novo fusion transcript assembly-based methods. Genome Biol. 2019;20(1):213.

8. Kerr DA, Pinto A, Subhawong TK, Wilky BA, Schlumbrecht MP, Antonescu CR, et al. Pericytoma With t(7;12) and ACTB-GLI1 fusion: reevaluation of an unusual entity and its relationship to the spectrum of GLI1 fusion-related neoplasms. Am J Surg Pathol. 2019;43(12):1682–92.

9. Panagopoulos I, Gorunova L, Rise TV, Andersen K, Micci F, Heim S. An Unbalanced chromosome translocation between 7p22 and 12q13 leads to ACTB-GLI1 fusion in pericytoma. Anticancer Res. 2020;40(3):1239–45.

10. Rollins BT, Cassarino DS, Lindberg M. Primary cutaneous epithelioid mesenchymal neoplasm with ACTB-GLI1 fusion: a case report. J Cutan Pathol. 2022;49(3):284–7.

11. Pettus JR, Kerr DA, Stan RV, Tse JY, Sverrisson EF, Bridge JA, et al. Primary myxoid and epithelioid mesenchymal tumor of the kidney with a novel GLI1-FOXO4 fusion. Genes Chromosomes Cancer. 2021;60(2):116–22.

12. Koh NWC, Seow WY, Lee YT, Lam JCM, Lian DWQ. Pericytoma with t(7;12): the first ovarian case reported and a review of the literature. Int J Gynecol Pathol. 2019;38(5):479–84.

13. Dahlen A, Fletcher CD, Mertens F, Fletcher JA, Perez-Atayde AR, Hicks MJ, et al. Activation of the GLI oncogene through fusion with the beta-actin gene (ACTB) in a group of distinctive pericytic neoplasms: pericytoma with t(7;12). Am J Pathol. 2004;164(5):1645–53.

14. Prall OWJ, McEvoy CRE, Byrne DJ, Iravani A, Browning J, Choong DY, et al. A malignant neoplasm from the jejunum with a MALAT1-GLI1 fusion and 26-year survival history. Int J Surg Pathol. 2020;28(5):553–62.

15. Argani P, Boyraz B, Oliva E, Matoso A, Gross J, Fridman E, et al. GLI1 gene alterations in neoplasms of the genitourinary and gynecologic tract. Am J Surg Pathol. 2022;46(5):677–87.

16. Alwaqfi RR, Samuelson MI, Guseva NN, Ouyang M, Bossler AD, Ma D. PTCH1-GLI1 fusion-positive ovarian tumor: report of a unique case with response to tyrosine kinase inhibitor pazopanib. J Natl Compr Canc Netw. 2021;19(9):998–1004.

17. Lyford-Pike S, Peng S, Young GD, Taube JM, Westra WH, Akpeng B, et al. Evidence for a role of the PD-1:PD-L1 pathway in immune resistance of HPV-associated head and neck squamous cell carcinoma. Can Res. 2013;73(6):1733–41.

18. Perry ME. The specialised structure of crypt epithelium in the human palatine tonsil and its functional significance. J Anat. 1994;185(Pt 1):111–27.

19. Bauwens L, Baltres A, Fiani DJ, Zrounba P, Buiret G, Fleury B, et al. Prevalence and distribution of cervical lymph node metastases in HPV-positive and HPV-negative oropharyngeal squamous cell carcinoma. Radiother Oncol. 2021;157:122–9.

20. Singer S, Socci ND, Ambrosini G, Sambol E, Decarolis P, Wu YS, et al. Gene expression profiling of liposarcoma identifies distinct biological types/subtypes and potential therapeutic targets in well-differentiated and dedifferentiated liposarcoma. Can Res. 2007;67(14):6626–36.

21. McConnell BB, Gregory FJ, Stott FJ, Hara E, Peters G. Induced expression of p16(INK4a) inhibits both CDK4- and CDK2-associated kinase activity by reassortment of cyclin-CDK-inhibitor complexes. Mol Cell Biol. 1999;19(3):1981–9.

22. Zhou C, Du J, Zhao L, Liu W, Zhao T, Liang H, et al. GLI1 reduces drug sensitivity by regulating cell cycle through PI3K/AKT/GSK3/CDK pathway in acute myeloid leukemia. Cell Death Dis. 2021;12(3):231.

23. Sigafoos AN, Paradise BD, Fernandez-Zapico ME. Hedgehog/GLI signaling pathway: transduction, regulation, and implications for disease. Cancers (Basel). 2021;13(14):3410.

24. Hutchison B, Sadigh S, Ferry JA, Shattuck TM, Faquin WC. Tonsillar p16-positive follicular dendritic cell sarcoma mimicking HPV-related oropharyngeal squamous cell carcinoma: a case report and review of reported cases. Head Neck Pathol. 2021;15(1):267–74.

25. Zhang L, Yang C, Lewis JS Jr, El-Mofty SK, Chernock RD. p16 expression in follicular dendritic cell sarcoma: a potential mimicker of human papillomavirus-related oropharyngeal squamous cell carcinoma. Hum Pathol. 2017;66:40–7.

26. Bishop JA, Rooper LM, Chiosea SI, Westra WH. Clear cell carcinoma of salivary glands is frequently p16 positive: a pitfall in the interpretation of oropharyngeal biopsies. Am J Surg Pathol. 2018;42(3):367–71.

27. Kanazawa T, Kodama K, Nokubi M, Gotsu K, Shinnabe A, Hasegawa M, et al. A case of solitary fibrous tumor arising from the palatine tonsil. Ear Nose Throat J. 2015;94(3):117–20.

28. Macarenco RS, Bacchi CE, Domingues MA. Solitary fibrous tumor with atypical histological features occurring in the palatine tonsil: an uncommon neoplasm in an uncommon site. J Oral Pathol Med. 2006;35(10):602–5.

29. Robinson DR, Wu YM, Kalyana-Sundaram S, Cao X, Lonigro RJ, Sung YS, et al. Identification of recurrent NAB2-STAT6 gene fusions in solitary fibrous tumor by integrative sequencing. Nat Genet. 2013;45(2):180–5.

30. Liang Y, Heller RS, Wu JK, Heilman CB, Tischler AS, Arkun K. High p16 expression is associated with malignancy and shorter disease-free survival time in solitary fibrous tumor/hemangiopericytoma. J Neurol Surg B Skull Base. 2019;80(3):232–8.

31. Antonescu CR, Agaram NP, Sung YS, Zhang L, Swanson D, Dickson BC. A distinct malignant epithelioid neoplasm with GLI1 gene rearrangements, frequent S100 protein expression, and metastatic potential: expanding the spectrum of pathologic entities with ACTB/MALAT1/PTCH1-GLI1 fusions. Am J Surg Pathol. 2018;42(4):553–60.